

On solutions of a Boussinesq-type equation with displacement-dependent nonlinearities: the case of biomembranes

[Jüri Engelbrecht](#), [Kert Tamm](#) and [Tanel Peets](#)

Centre for Nonlinear Studies, Institute of Cybernetics at Tallinn University of Technology, Akadeemia tee 21, Tallinn 12618, Estonia

ABSTRACT

Boussinesq-type wave equations involve nonlinearities and dispersion. In this paper a Boussinesq-type equation with displacement-dependent nonlinearities is presented. Such a model was proposed by Heimbürg and Jackson (2005) for describing longitudinal waves in biomembranes and later improved by Engelbrecht et al. (2015) taking into account the microinertia of a biomembrane. The steady solution in the form of a solitary wave is derived and the influence of nonlinear and dispersive terms over a large range of possible sets of coefficients demonstrated. The solutions emerging from arbitrary initial inputs are found using the numerical simulation. The properties of emerging trains of solitary waves are analysed. Finally, the interaction of solitary waves which satisfy the governing equation is studied. The interaction process is not fully elastic and after several interactions radiation effects may be significant. This means that for the present case the solitary waves are not solitons in the strict mathematical sense. However, like in other cases known in solid mechanics, such solutions may be conditionally called solitons.

KEYWORDS

elastic waves; lipids; mechanical behaviour, nonlinearities; dispersion; solitary waves

1. Introduction

The celebrated wave equation which is based on the conservation of momentum, models the motion with a finite speed. In order to account for accompanying physical phenomena, the wave equation must be modified. For conservative systems, the Boussinesq-type equations are widely used. The original Boussinesq equation was derived for surface waves on a fluid layer [1, 2] but nowadays such equations are used also in solid mechanics [3]. The main features of Boussinesq-type equations are: (i) bi-directionality (d'Alembert operator); (ii) nonlinearity of any order; (iii) dispersion of any order (presence of space and time derivatives of the fourth order or higher [3]). Beside fluid mechanics, there are many studies of such equations derived using various physical assumptions [3–8, etc]. In solid mechanics, nonlinearity is caused by the nonlinear stress-strain relation and the nonlinear strain tensor, i.e., physical and geometrical nonlinearities are involved (see, for example, [9]). The governing equations involve then $\partial u_i / \partial x_j$ type terms ($i, j = 1, 2, 3$), i.e., the displacement gradients enter

the model. For example, the simple 1D equation reads

$$u_{tt} - c_0^2(1 + ku_x)u_{xx} = 0, \quad (1)$$

where $u = u_1$, $x = x_1$, c_0 is the velocity in the unperturbed state and k is the nonlinear parameter. Here and further, the indices x and t denote the differentiation with respect to the indicated variable. One could say that actually the effective velocity c_e is calculated like

$$c_e^2 = c_0^2(1 + ku_x). \quad (2)$$

The dispersive effects in solids are due to the geometry [6] or due to the microstructure [7, 10, etc]. Then terms like u_{xxxx} , u_{xxtt} etc. appear in governing equations. The combined action of nonlinear and dispersive effects may give rise to solitary waves [3, 11, 12, etc].

During the last decade the interest to mechanical waves in biomembranes has been growing [13–15, etc]. The biomembranes have a special structure, made of lipids [13, 16] and in this case nonlinearities are different from that in solids. Based on experimental results, the nonlinearity in biomembranes can be accounted in the effective velocity c_e like [13]

$$c_e^2 = c_0^2 + pu + qu^2, \quad (3)$$

where p and q are coefficients, c_0 is the velocity of the small amplitude sound wave and u is the density change along the axis of the biomembrane. This means that contrary to the gradient-type nonlinearity, the displacement-type nonlinearity appears in governing equations for waves in biomembranes. The Heimburg-Jackson (HJ) model [13], improved by Engelbrecht et al. [8] takes such nonlinearities into account together with dispersive term(s). The governing equation is then of the Boussinesq-type and may lead to the emergence of solitary waves.

In this paper, the improved Heimburg-Jackson model [8] is systematically studied in detail needed for describing the possible emergence of solitary waves. After describing the derivation of the governing Boussinesq-type equation (Section 2), the following questions are analysed: (i) deriving the steady solutions to the governing equation (Section 3); (ii) finding the solutions for an arbitrary input (Section 4); (iii) studying the interaction of waves (Section 5). In this way, the existence of solitary waves is shown, the emergence of trains of solitary waves is demonstrated, and finally, the interaction of solitary waves shows whether the solitary waves are solitons in the classical sense. As it is well known, solitons interact with each other elastically without losses like elementary particles and only the phase shifts show the interaction effects [17–19]. In many physical systems the interaction is accompanied by radiation, i.e., the process is not fully elastic. In this case the solitary waves can only conditionally be called solitons. The final remarks are presented in Section 6 where the special features of solutions to this Boussinesq-type equation with displacement-dependent nonlinearities are summarised. The analysis is wider than only the case of biomembranes and includes many combinations of governing parameters.

2. Derivation of the governing equation

The signal propagation in a nerve fibre is a complicated phenomenon. The nerve fibre itself can be modelled as a tube filled with axoplasm and surrounded by the extracellular fluid. The wall of the tube is made of a biomembrane [20]. The biomembrane is a very special biological structure made of phospholipids with hydrophobic tails directed to inside of the membrane, i.e., away from the intra- and extracellular fluid [16]. In general, the lipid membrane represents a special biological microstructure with complicated properties. The concentration of ions within and outside of a fibre is different but the ion change can occur through the ion channels. These channels are closed at the rest but can be opened under electrical or mechanical impact [16].

The electrophysiological model describing the propagation of an electrical signal called the action potential was derived by Hodgkin and Huxley [21] and is based on telegraph equations and on opening and closing the ion channels under the electrical impact. However, this model cannot explain all the complex effects in the nerve fibres. Experiments by Iwasa et al. [22] and Tasaki [23] have clearly demonstrated the swelling of the surrounding biomembrane and the accompanying heat exchange. This means that an action potential is accompanied also by a mechanical wave in the fibre wall. A mathematical model governing such a wave is proposed by Heimburg and Jackson [13, 24]. Their model is based on the wave equation, i.e., on the balance of momentum and written in terms of density change $\Delta\rho_A = u$ in the longitudinal direction:

$$u_{tt} = (c_e^2 u_x)_x. \quad (4)$$

Two essential assumptions are made. First, it is assumed that the velocity c_e of a wave in a circular biomembrane is related to the compressibility of the lipid structure and can be taken as in Eq. (3) ($c_e^2 = c_0^2 + pu + qu^2$) and the second assumption is to add *ad hoc* higher order term to the governing equation $-hu_{xxxx}$ responsible for dispersion [13]. The governing equation is then

$$u_{tt} = [(c_0^2 + pu + qu^2)u_x]_x - hu_{xxxx}, \quad (5)$$

where h is a constant. Equation (5) is a Boussinesq-type equation [3]. Heimburg and Jackson [13] have demonstrated that Eq. (5) possesses a solitary pulse-type solution. There are several further studies analysing such solutions [14, 15, 24, etc]. Equation (5) has been improved by Engelbrecht et al. [8] in order to remove the discrepancy that at higher frequencies the velocities are unbounded. Following the ideas from the solid mechanics [7, 10] and supported by the Lagrangian formalism, the inertial term is added to the governing equation:

$$u_{tt} = [(c_0^2 + pu + qu^2)u_x]_x - h_1 u_{xxxx} + h_2 u_{xxtt}, \quad (6)$$

where $h_1 = h$ and h_2 are dispersion coefficients.

The importance of the additional dispersion term $h_2 u_{xxtt}$ can be explained with dispersion analysis. It has been shown in [8] that in case of only one dispersion term $h_1 u_{xxxx}$ (Eq. (5)), the phase velocity is expressed as $c_{ph}^2 = c_0^2 + h_1 k^2$ and it tends to infinity as the wave number k is increased. In case of the second fourth order mixed dispersion term $h_2 u_{xxtt}$ the propagation velocity is bounded as it can be seen in Fig. 1. The bounding velocity c_1 for high frequency harmonics is defined by the ratio of the dispersion coefficients ($c_1^2 = h_1/h_2$) and the coefficient h_2 is related to the rate

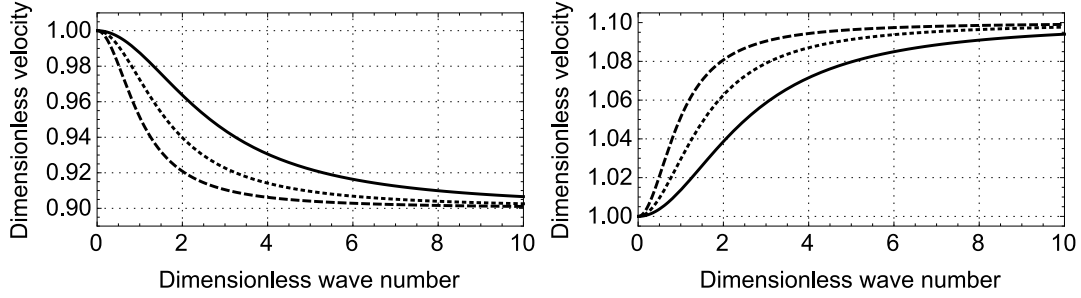


Figure 1. Phase speed curves for Eq. (6) in case of $c_1/c_0 = 0.9$ (left figure) and $c_1/c_0 = 1.1$ (right figure). $h_2/c_0^2 = 1$ (dashed), $h_2/c_0^2 = 0.4$ (dotted line) and $h_2/c_0^2 = 0.15$ (solid line) in both figures.

of change of the velocity from low frequency to the high frequency domain. Higher valued coefficient h_2 means that the transition from the low frequency speeds to the higher frequency speed is more rapid (see Fig. 1). We also note that $c_1/c_0 < 1$ means normal dispersion, i.e., the higher frequency harmonics travel slower than the lower frequency harmonics and $c_1/c_0 > 1$ means anomalous dispersion.

From the viewpoint of solid mechanics the importance of the fourth order mixed derivative is not surprising as it is well known that the presence of only spatial derivatives in the governing equation can lead to instabilities [5]. Moreover, the mixed fourth order derivative is related to the inertia of the microstructure and it is shown by Maurin and Spadoni [25] that both dispersive terms arise naturally as a result of proper modelling and this has also been demonstrated experimentally [26].

The focal point of this paper is the full analysis of Eq. (6). Further it is convenient to use the dimensionless form of Eq. (6), which will take the form

$$U_{TT} = (1 + PU + QU^2)U_{XX} + (P + 2QU)U_X^2 - H_1U_{XXXX} + H_2U_{XXTT}, \quad (7)$$

where $X = x/l$, $T = c_0t/l$, $U = u/\rho_A$ and $P = p\rho_A/c_0^2$, $Q = q\rho_A^2/c_0^2$. Here l is a certain length, for example, the fibre diameter.

Equation (7) must be solved under initial and boundary conditions formulated in the dependent variable U .

3. Steady solutions

In this Section we focus our analysis on undistorted travelling waves in the form

$$V = V(\xi), \quad \xi = X - cT, \quad (8)$$

where V is some function and c is dimensionless wave velocity [18, 27]. Substituting this into Eq. (7) we get

$$c^2V'' = ((1 + PV + QV^2)V')' - H_1V'''' + H_2c^2V'''''. \quad (9)$$

Integrating Eq. (9) twice we get after some rearranging

$$(H_1 - H_2c^2)V'' = (1 - c^2)V + \frac{1}{2}PV^2 + \frac{1}{3}QV^3 + A\xi + B, \quad (10)$$

where A and B are constants of integration. Since we are looking for solitary wave solutions, then we may add boundary conditions that $V, V', V'' \rightarrow 0$ as $X \rightarrow \pm\infty$ and therefore $A, B = 0$ [18, 27]. Now the Eq. (10) is multiplied by V' and integrated to get

$$(H_1 - H_2c^2)(V')^2 = (1 - c^2)V^2 + \frac{1}{3}PV^3 + \frac{1}{6}QV^4, \quad (11)$$

which can be rewritten as

$$(H_1 - H_2c^2)(V')^2 = \Phi_{eff}(V), \quad (12)$$

where

$$\Phi_{eff}(V) = (1 - c^2)V^2 + \frac{1}{3}PV^3 + \frac{1}{6}QV^4 \quad (13)$$

is a fourth-order ‘pseudo-potential’. Note that for the classical KdV equation the ‘pseudo-potential’ is of the third order [18]. While the KdV equation involves the quadratic nonlinearity then taking also the cubic nonlinearity into account, the result is an expanded KdV equation called the Gardner equation [28]. For the Gardner equation the ‘pseudo-potential’ is of the fourth order which leads to a solitonic solution [29]. The difference between KdV-type evolution equations and Boussinesq-type wave equations is explained earlier [30].

The existence of solitary waves can be analysed by either investigating the behaviour of the ‘pseudo-potential’ (13) or the phase portrait of Eq. (11). In case of $H_2 = 0$ the ‘pseudo-potential’ (13) also applies for the Heimbürg-Jackson model (5) and has been analysed by Lautrup et al. [31] for a particular set of parameters that were determined experimentally and are relevant for the solitary wave propagation in biomembranes ($P < 0, Q > 0$). Here the analysis is more general and the signs of the parameters P and Q are not fixed.

The four zeros of the polynomial (13) are

$$V_{1,2} = 0 \quad \text{and} \quad V_{3,4} = \frac{P}{Q} \left(-1 \pm \sqrt{1 - \frac{(1 - c^2)6Q}{P^2}} \right). \quad (14)$$

If $c^2 < 1$ and $H_1 - H_2c^2 > 0$ (or the other way around) then the double zero at $V_{1,2} = 0$ indicates the saddle point, which is minimal requirement for the existence of solitary waves [18, 27]. The following analysis can be divided into two parts: the cases of $H_1 - H_2c^2 > 0$, which has also been analysed previously [30] and $H_1 - H_2c^2 < 0$. Attention is paid to the signs of P and Q which govern the structure of solutions.

(i) $H_1 - H_2c^2 > 0$

The case of $Q > 0$. For this case the analysis is pretty straightforward. It can be deduced from aforementioned restrictions and from Eq. (14) that in this case the additional condition for the velocity c is

$$1 > |c| > \sqrt{1 - \frac{P^2}{6Q}} \quad (15)$$

which means that in case of $Q > 0$ and $H_1 - H_2c^2 > 0$ the solitary waves governed by the Eq. (7) will always travel slower than the low frequency sound. This is in good

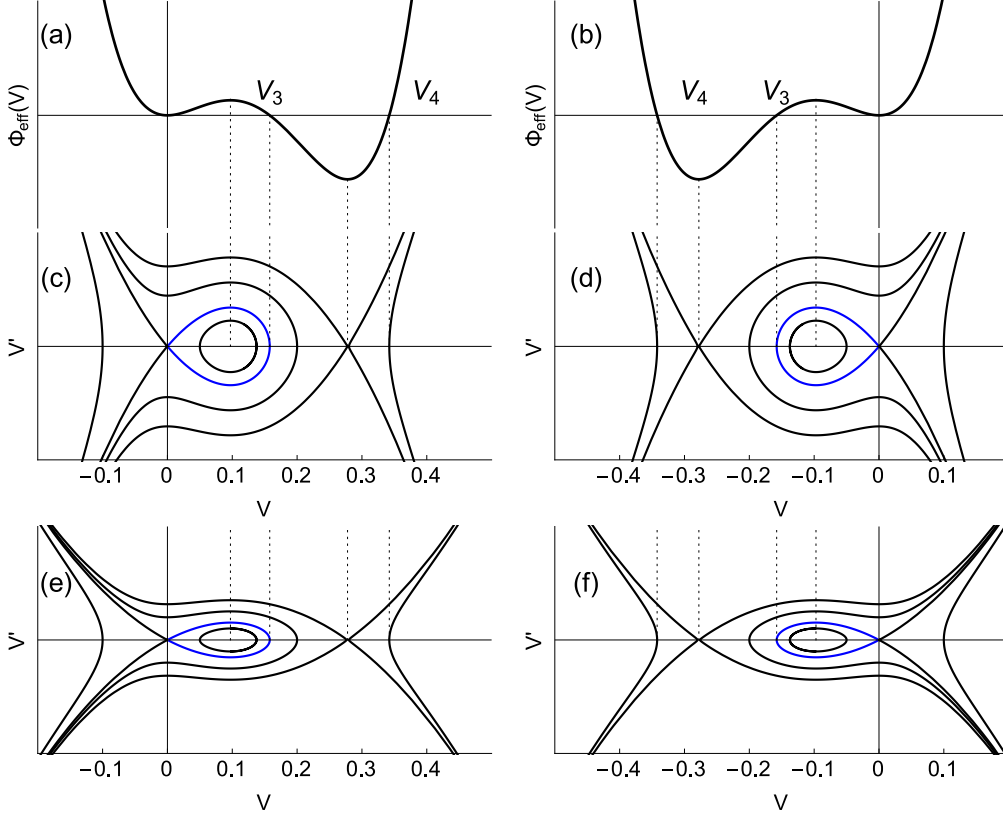


Figure 2. Shape of the ‘pseudopotential’ (13) and phase portrait of Eq. (11) in case of $Q > 0$. Here $c = 0.8$, $Q = 40$, $|P| = 10$, $H_1 = 4$, while $H_2 = 5$ for the middle panels and $H_2 = 0$ for the bottom panels. Homoclinic orbit is shown in blue.

agreement with the actual pulse propagation in biomembranes [13, 31].

The ‘pseudopotential’ (13) and the corresponding phase portrait for this case have been plotted in Fig. 2 for $P < 0$ (left column) and for $P > 0$ (right column), respectively. The ‘pseudopotential’ (13) is plotted in the top row and the phase portraits for the case $H_2 \neq 0$ in the middle and for the case $H_2 = 0$ is plotted in the bottom row for reference. It is clearly seen that the cases of $H_2 \neq 0$ and $H_2 = 0$ are topologically equivalent, but the changes in the derivative V' is clearly seen.

The existence of solitary wave solution requires that $\Phi_{eff}(V)$ has a local minimum at $V = 0$ with at least one local maximum next to it (Figs 2a,b). Alternatively one can study the phase portrait (Figs 2c,d): solitary wave solutions exist when a saddle point and a homoclinic orbit exists (shown in blue). The amplitude of the solitary wave in both cases is determined by V_3 . It is clear that while the magnitude of the amplitude of a solitary wave depends on the ratio of the parameters P and Q together with the velocity c , the sign of the amplitude is determined only by the parameter P : in case of $P < 0$ positive solitary wave emerges and in case of $P > 0$ the amplitude will be negative. It can also be shown that higher values of c result in lower amplitudes meaning that the lower amplitude solitary waves travel faster as it has been shown earlier [32, 33].

The case of $Q < 0$ is shown in Fig. 3, where it can be seen that the behaviour of the ‘pseudopotential’ and the phase portrait is significantly different from the case of $Q > 0$, $H_1 - H_2c^2 > 0$. Since there are two regions where $\Phi_{eff}(V) > 0$, two solitary

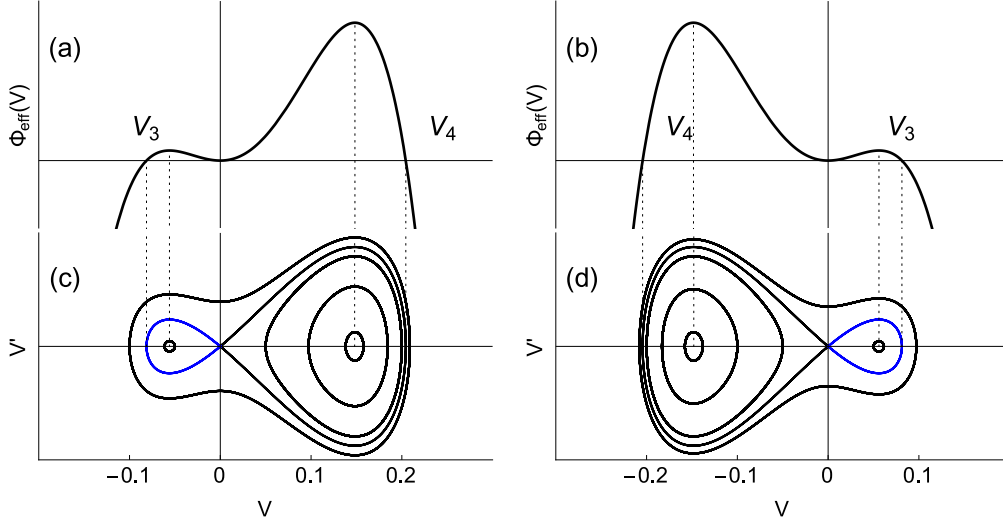


Figure 3. Shape of the ‘pseudopotential’ (13) and phase portrait of Eq. (11) in case of $Q < 0$. Here $c = 0.8$, $Q = -130$, $|P| = 8$, $H_1 = 4$ and $H_2 = 5$. Homoclinic orbit for solution (17) is shown in blue.

waves with opposite polarities can coexist. The condition for the velocity c is

$$1 > |c| > 0 \quad (16)$$

meaning that also in this case the solitary wave travels slower than the speed of the low frequency sound. As in case of $Q > 0$, here also the magnitude and the sign of the amplitude is determined by the parameters P , Q and c and the higher velocities c result in larger negative amplitudes.

Recalling that the analytical solution of Eq. (7) is [30, 34]

$$u(\xi) = \frac{6(c^2 - 1)}{P(1 + \sqrt{1 + 6Q(c^2 - 1)/P^2 \cosh(\xi\sqrt{(1 - c^2)/(H_1 - H_2c^2)})})}, \quad (17)$$

where $\xi = X - cT$ and c is the velocity of the solitary wave, the solitary wave solutions for the given cases are plotted in Fig. 4 where the solid lines represent the case of $H_2 \neq 0$ and the dashed represents the case of $H_2 = 0$, which is the original Heimbürg-Jackson equation (5). We also note that in case of Eq. (17) only solitons with amplitude V_3 is realised for both cases.

In addition, it can be seen in Figs. 2 and 3 that in addition to the homoclinic orbits also periodic orbits exist and such solutions can arise from the suitable initial conditions. Such a situation will be discussed in Section 4.

Although solitary waves in case of $Q < 0$ and $H_1 - H_2c^2 > 0$ exist only when $0 < c < 1$, periodic solutions to Eq. (11) also exist when

$$1 < |c| < \sqrt{1 + \left| \frac{P^2}{6Q} \right|}. \quad (18)$$

This case is demonstrated in Fig. 5 where it can be seen that in this case ‘pseudopotential’ (13) is positive between the points V_3 and V_4 and a stable orbit exists (shown in blue) which means an existence of a periodic solution. What is interesting is that

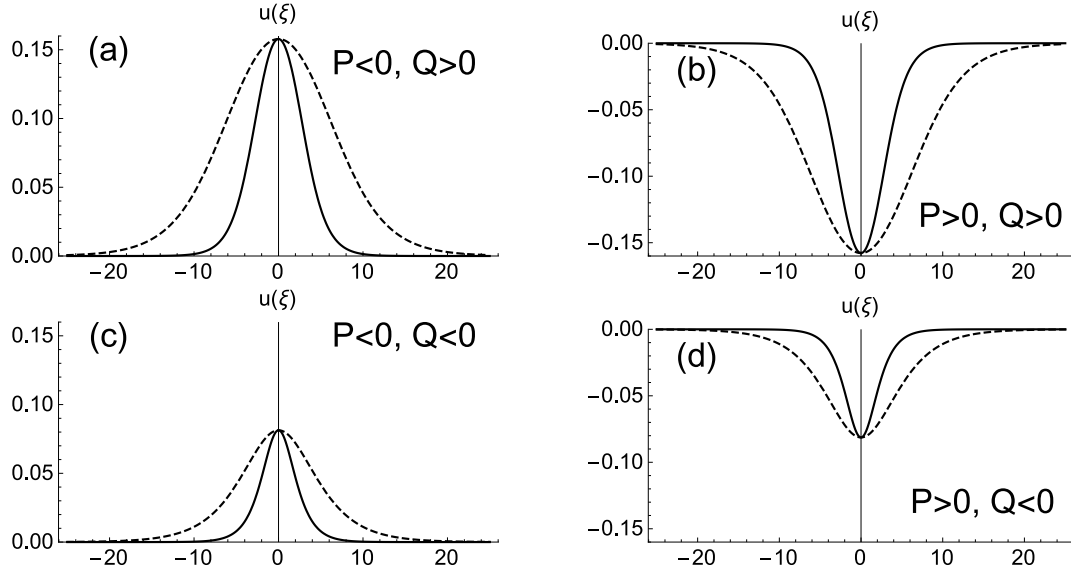


Figure 4. Solitary wave solutions of Eq. (7) in case of $H_2 \neq 0$ (solid line) and $H_2 = 0$ (dashed line). Here $|P| = 16, |Q| = 80$ (top row) and $|P| = 8, |Q| = 130$ (bottom row); $c = 0.8, H_1 = 2, H_2 = 5$ for all plots.

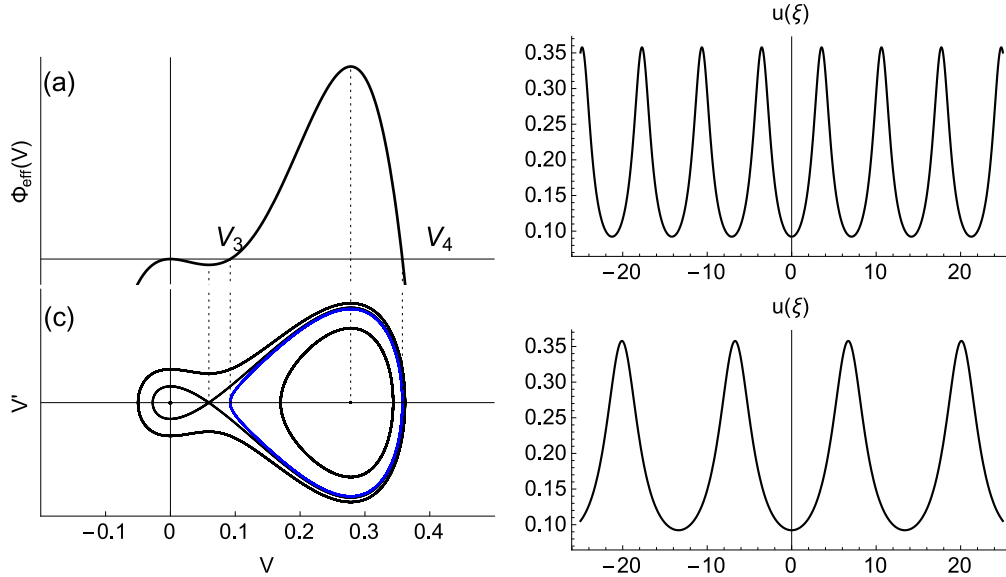


Figure 5. Emergence of a periodic wave in case of $Q < 0, H_1 - H_2c^2 > 0$ and $c > 1$: the shape of the ‘pseudopotential’ (a) and the corresponding phase portrait (c). For (b) the parameters are $c = 1.2, Q = -80, P = 18, H_1 = 2, H_2 = 1$. For (d) $H_2 = 20$; other parameters are same as in (b). Stable orbit is shown in blue.

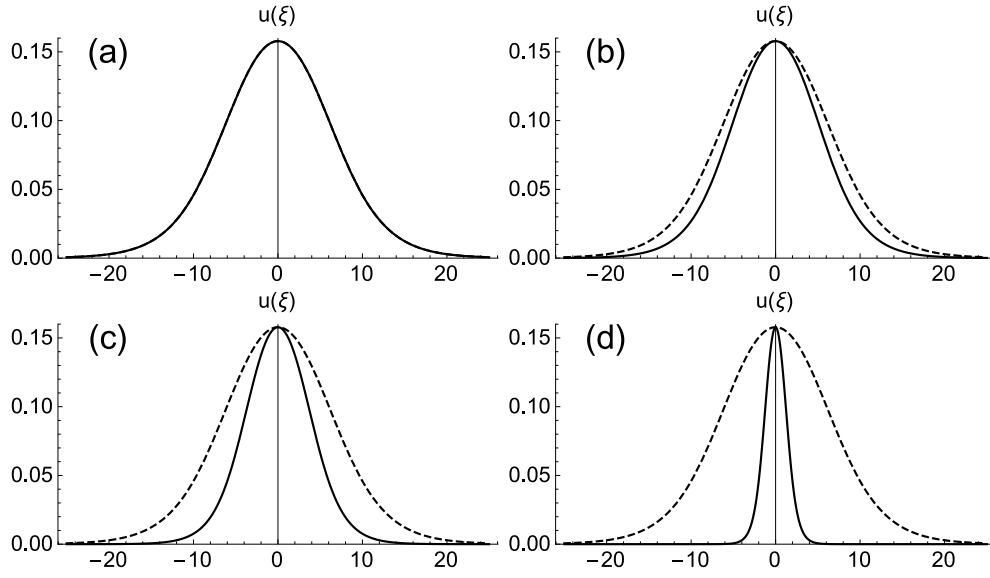


Figure 6. The effect of the second dispersive term H_2U_{XXTT} on the width of a solitary wave. Here $P = -10$, $Q = 40$, $H_1 = 2$; (a) $H_2 = 0$, (b) $H_2 = 2$, (c) $H_2 = 4$ and (d) $H_2 = 6$.

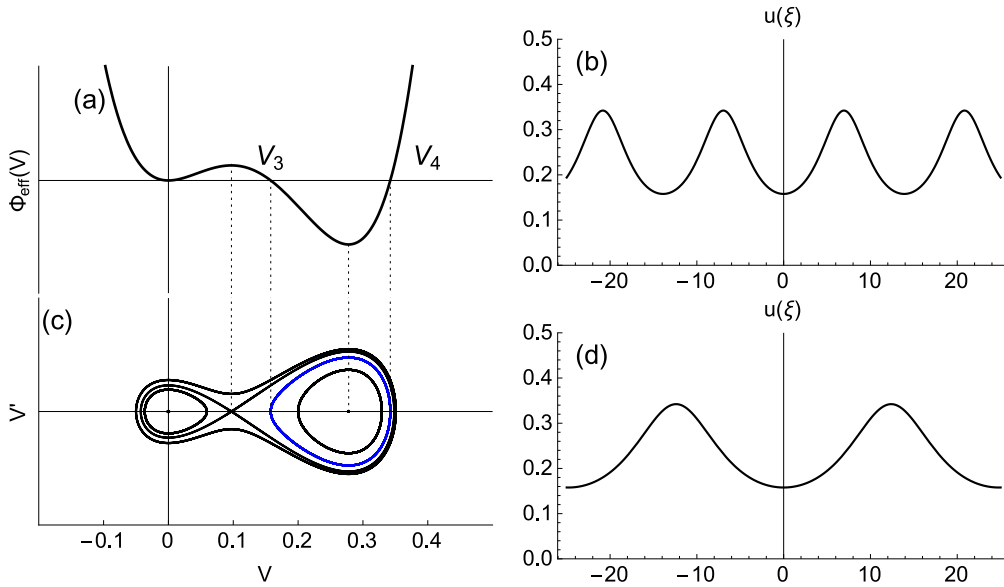


Figure 7. Emergence of a periodic wave in case of $H_1 - H_2c^2 < 0$: the shape of the ‘pseudopotential’ (a) and the corresponding phase portrait (c). For (b) the parameters are $c = 0.8$, $Q = 40$, $P = -10$, $H_1 = 4$, $H_2 = 9$. For (d) $H_2 = 20$; other parameters are same as in (b). Stable orbit for solution (17) is shown in blue.

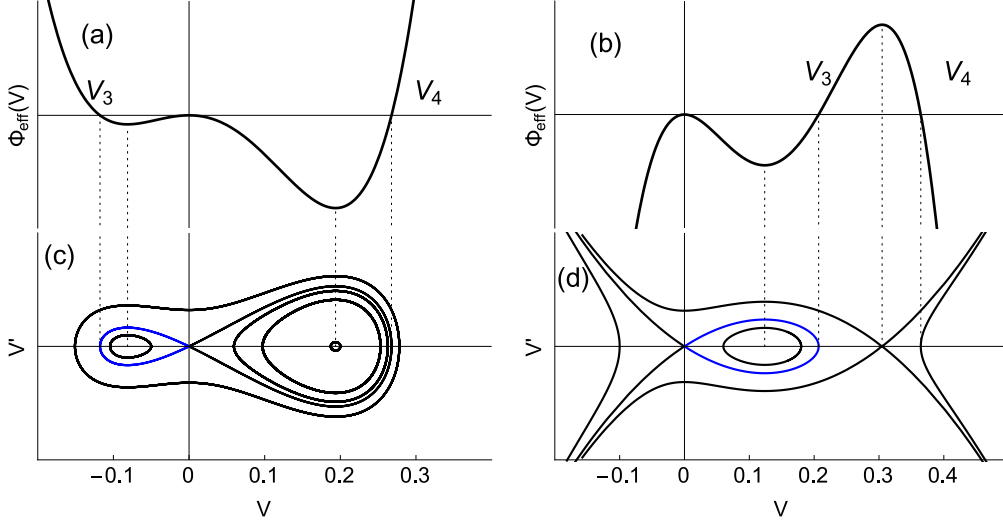


Figure 8. Existence of solitary waves in case of $H_1 - H_2c^2 < 0$ and $c > 1$. Here $c = 1.1$, $Q = 40$, $P = -3$, $H_1 = 4$ and $H_2 = 5$ (left column) and $c = 1.2$, $Q = -35$, $P = 10$, $H_1 = 4$ and $H_2 = 5$ (left column). Homoclinic orbit for solution (17) is shown in blue.

the phase portrait in this case looks similar to Fig. 3c only it has been slightly shifted to the right and the higher amplitude part is realised.

It can also be seen in Figs 2, 3 and 4 that in the case of the second dispersion coefficient H_2 a more localised solution is obtained: the greater value of the quantity V' means the steeper slope (and hence the smaller width) of the solitary wave. The effect of the dispersive term H_2 on the width of a solitary wave is demonstrated in Fig. 6, where it can be seen that higher values of H_2 result in more localised solutions.

(ii) $H_1 - H_2c^2 < 0$

Since Eq. (11) can be thought of as conservation of ‘pseudoenergy’, then if condition $H_1 - H_2c^2 < 0$ is satisfied then also Φ_{eff} has to be negative. In case of $Q > 0$ the condition $H_1 - H_2c^2 < 0$ means that periodic solutions emerge even in the case of $c < 1$ as it is seen in Fig. 7. Here also the periodic solution oscillates between the values V_3 and V_4 (shown in blue in Fig. 7), which corresponds to the region where $\Phi_{eff}(V) < 0$ as it can be seen in Fig. 2a. Similar result is obtained when $P > 0$, only with negative amplitude.

In case of $c > 1$ and $Q > 0$ the ‘pseudopotential’ will only have regions $\Phi_{eff} < 0$ and in case of $H_1 - H_2c^2 < 0$ a solitary wave with amplitude V_3 exists (Fig. 8a,c). Similarly, in case of $c > 1$ and $Q < 0$, a solitary wave with amplitude V_3 exists (Fig. 8b,d). Like in previous cases the structure of the phase portrait depends on the sign of the coefficient Q and the sign of V_3 (amplitude of the solution) depends on the sign of the coefficient P . Unlike in case of $H_1 - H_2c^2 > 0$ where smaller amplitude solitary waves travel faster, in case of $H_1 - H_2c^2 < 0$ the higher amplitude waves travel faster. Also recall that if $H_1 - H_2c^2 > 0$ then periodic solution exists with the same coefficients (see Fig. 5).

Last case we mention is $H_1 - H_2c^2 < 0$, $c < 1$ and $Q < 0$ when no solitonic solutions exist.

4. Solutions emerging from arbitrary initial conditions

In the present paper we use the pseudospectral method (PSM) to solve the governing equation (7) under localised initial conditions demonstrating the influence of parameters P, Q, H_1 and H_2 on the evolution of solutions. The PSM is a well established method which is used for solving PDE's and ODE's on regular basis. The advantages and disadvantages of the PSM are well explored in the literature [35, 36]. Here two points are worth of highlighting: (i) the PSM requires one to use periodic boundary conditions, (ii) the governing equations have to be in a suitable form for applying the PSM with time derivatives on the left hand side and spatial derivatives on the right hand side of the equation. The first point is not a problem, however, taking a look at Eq. (7) it is evident that we have a mixed partial derivative term U_{XXTT} . We use a change of variables for transforming the governing equation (7) for allowing the application of the PSM [8, 32, 33]. The basic idea of the PSM is to find the spatial derivatives by making use of the properties of the Fourier transform and then solve the resulting ODE with respect to time derivative by making use of the commonly available schemes for numerical solving of the ODE's.

For initial and boundary conditions for the systematic analysis we use a pulse-type localised initial condition in the form of sech^2 -type profile: $U(X, 0) = U_o \text{sech}^2 B_o X$, $U(X, T) = U(X + 2km\pi, T)$, $m = 1, 2, \dots$, where $k = 12$, i.e., the total length of the spatial period is 24π . Here the amplitude and the width of the initial pulse are $U_o = 1$ and $B_o = 1$. The initial phase velocity is $U(X, 0)_T = 0$ meaning that the initial condition splits into two pulses propagating in the opposite directions. Some examples are provided using different combinations of parameters in which case the used parameters are noted separately. Although the initial condition is strictly speaking not a periodic function and first derivatives jump across the boundary point, the numerical error using the PSM with such a periodic boundary condition is small. This is clearly demonstrated in the detailed analysis of the applicability of the PSM [37].

The calculations are carried out with the Python package SciPy [38] with Python interface to the ODEPACK FORTRAN code [39] for the ODE solver.

In addition to the formation of solitary waves a number of different waveprofile regimes exist for the solutions of the governing equations (7) depending on the parameters but also on the initial conditions. To name the ones investigated previously:

- (i) solitary waves (single or as a part of solitary wave train, see Figs 9,10);
- (ii) Airy or reverse Airy like oscillatory structures (see Fig. 9);
- (iii) hybrid solution where part of the initial pulse evolves into a train of solitary waves and remainder of the initial pulse forms an oscillatory structure [32–34].

From the viewpoint of nerve pulse propagation the most interesting one is the solitary wave solution, however, the rest of the solution types can not be ignored either as these might be relevant somehow for either nerve pulse propagation or some kind of pathologies. It should be emphasised that not only the equation parameters are important in determining what kind of solution evolves from the initial excitation but also the character of an initial excitation is important. As an example see Fig. 9 where some solutions corresponding to the different parameters and initial condition amplitudes are presented. Depending on the dispersion type the initial excitation sign determines whether the emerging wave structure is composed of solitary pulses or Airy or reverse-Airy type oscillatory packet under the parameter combination used in Fig. 9. Another interesting phenomenon which must be mentioned is the case where smaller amplitude solitary waves can travel faster than the high amplitude ones as

can be seen in Fig. 10. Under the suitable parameter combinations it is possible to observe solutions where both negative and positive amplitude solitary waves can exist simultaneously and if the smaller amplitude solitary waves travel faster then the larger negative amplitude solitary waves travel even faster. However, this is not an universal symmetry but needs the right ratio of parameters. The most common solution type seems to be an oscillatory structure with few solitary pulses where some part of the initial pulse energy is sufficient to form one or more solitary pulses and the remainder forms an oscillatory trail either in front or behind (depending of the dispersion type) of the propagating solitary waves.

In Fig. 11 an example of contour plots with isoline interval of 0.05 from -0.4 to $+1$ for the amplitude is presented.

In addition we are tracking waveprofile peak trajectories by finding the exact local maxima of the wave profiles by making use of the properties of the Fourier transform [37] (reconstructing the wave profile from the Fourier spectrum to minimise inaccuracies from using the discrete grid) for finding the exact spatial coordinates of the pulse peaks at each time step for the purposes of finding the waveprofile velocities. Following observations follow from such an analysis:

(i) the dispersion parameters have a strong effect on the evolution of the wave profiles – the main pulse velocities are clearly different depending on the dispersion parameters and in addition the dispersion type determines on which side (relative to the propagation direction) the secondary wave structures emerge from the main pulse. Increasing the parameter H_1 increases the main pulse propagation velocity as predicted by dispersion analysis [32];

(ii) The nonlinear parameters P and Q have some influence on the waveprofile propagation velocities. In the case of the normal dispersion ($c_1/c_0 < 1$) increasing the nonlinearity leads to the slower propagation velocity for the wave profiles. In the case of the anomalous dispersion ($c_1/c_0 > 1$) the main pulse velocity remains almost the same, however, the effect is more significant for the secondary oscillatory structures meaning that in the case of higher nonlinear parameters the secondary structures have propagated at higher velocity. This is in agreement with previous results where it has been demonstrated that due to the uncommon (in the context of Boussinesq type equation) nonlinear terms certain parameter combinations can exist where the smaller amplitude solitary waves propagate faster than the higher amplitude ones [33].

Next, let us take a more detailed look how the the nonlinear and dispersive parameters influence the observable quantities of the wave profiles under the positive and negative initial conditions. We observe the speed of the peak of the main pulse. We track the coordinates of the peak of the main pulse by reconstructing the waveprofile shape from the full Fourier spectrum at each time step. Parameters P and Q change from -0.9 to $+0.9$ with the step size of 0.1 and for dispersion related parameters H_1 and H_2 three combinations are recorded – an normal dispersion case ($H_1 = 0.3, H_2 = 0.7$), ‘balanced dispersion’ case ($H_1 = H_2 = 0.5$) and anomalous dispersion case ($H_1 = 0.7, H_2 = 0.3$).

The notation of ‘balanced dispersion’ needs some clarification as it is not in common use like anomalous and normal dispersion type are. In essence it is a a situation where two dispersion terms in governing equation have opposite signs and their influence is balanced resulting only in slight (almost unnoticeable) dispersion in wave profiles. It must be stressed that this is not a dispersionless case.

Although for biomembranes the nonlinear parameters fulfil the conditions $P < 0, Q > 0$ [13], from the viewpoint of general analysis the other variants are also possible. The case $P < 0, Q > 0$ leads to following conclusions:

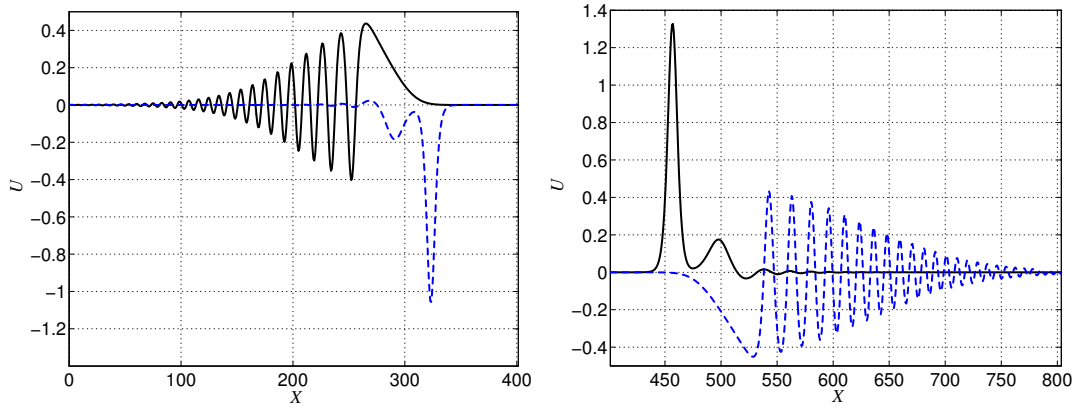


Figure 9. Waveprofile plots in the normal (left, $T = 1500$) and anomalous (right, $T = 1700$) dispersion cases for the positive (solid black line) and negative (blue dashed line) initial condition amplitudes. Waveprofile propagation direction is from left to right. Parameters: $U_o = \pm 1$, $B_o = 1/8$, $k = 128$, $n = 1024$, $c_o = 1$, $P = -0.1$, $Q = 0.01$, $H_2 = 0.5$ and $H_1 = 0.28125$ (normal dispersion), $H_1 = 0.78125$ (anomalous dispersion).

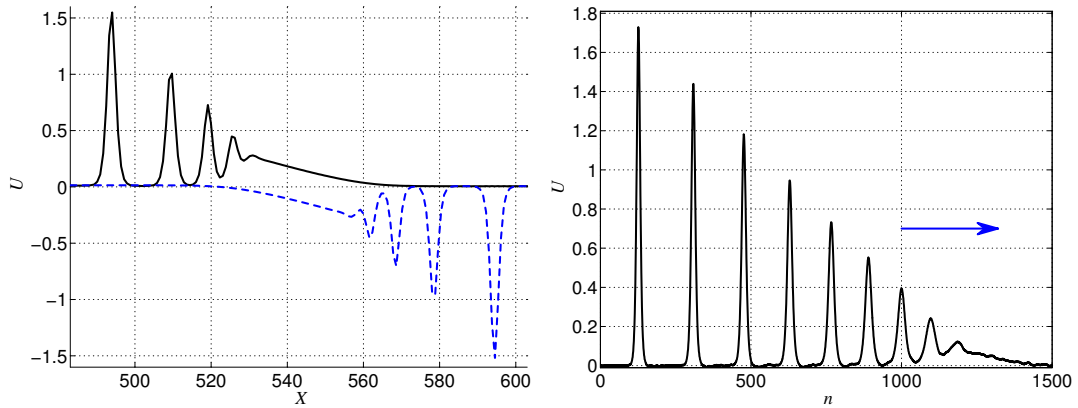


Figure 10. Waveprofiles comparison plot (left) at $T = 1750$ for the negative (blue dashed line) against positive (black solid line) initial condition amplitude. Lower amplitude solitary waves propagating faster. Direction of propagation from left to right. Parameters: $P = -0.1$, $Q = 0.05$, $H_1 = 0.5$, $H_2 = 0.5$, $k = 128$, $n = 1024$, $U_o = \pm 1$, $B_o = 1/8$, $c_o = 1$, $T = 0 \dots 1750$. Example of evolved solitary wave train is plotted on the right [33].

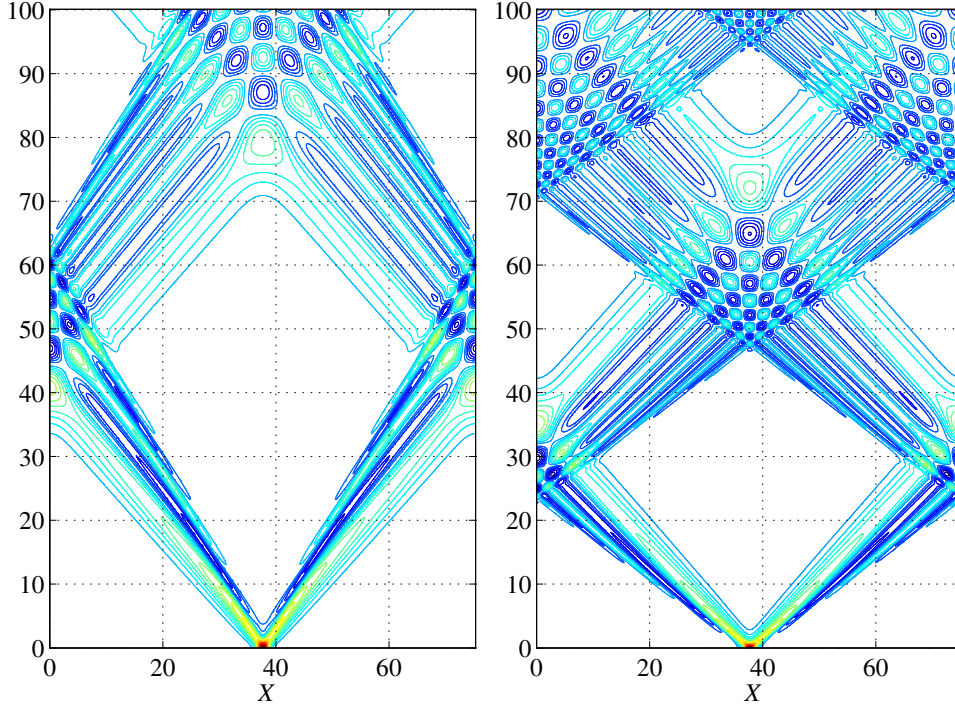


Figure 11. The waveprofile contour plots for $P = -0.1$, $Q = 0.1$ and normal dispersion ($H_1 = 0.3$, $H_2 = 0.7$, left) and anomalous dispersion ($H_1 = 0.7$, $H_2 = 0.3$, right) cases. Positive initial amplitude. Amplitude isoline interval 0.05 from -0.4 to $+1$, colourmap from blue (negative) to red (positive). Time T on vertical axis.

Normal dispersion case. The negative amplitude initial condition leads to a greater main pulse velocity than the positive amplitude initial condition. Under the both initial condition signs decreasing the nonlinear parameter Q (towards the zero) leads to a small decrease of the main pulse velocity. In the case of the negative amplitude initial condition the main pulse amplitude is greater than in the case of the positive amplitude initial condition and the observed oscillations are larger for the case with positive initial amplitude than in the case with the negative initial amplitude. Increasing parameter P leads to decrease in the main pulse velocity in the case of the negative amplitude initial condition while in the case of the positive initial amplitude the main pulse velocity remains the same. Increasing parameter P towards zero leads to marginally greater amplitude for the main pulse in the case of negative amplitude initial condition while in the case of positive initial amplitude the main pulse amplitude is unaffected by the changes in the nonlinear parameter P . The oscillatory structure magnitude is unaffected in the normal dispersion case.

Anomalous dispersion case. The main pulses propagate with velocity greater than one under both of the considered initial condition signs, however, the main pulse amplitudes and associated oscillatory structures are different. Increasing the parameter Q leaves the observed propagation speed the same but decreases the observed main pulse amplitude and leaves the observed oscillatory structures about the same. Increasing the parameter P does not affect the main pulse velocity significantly in the considered dispersion case regardless of the sign of the initial amplitude. However, increasing the nonlinear parameter P , the main pulse amplitude will be decreased and the amplitude of the oscillatory structures will be increased under the both considered signs of the initial condition.

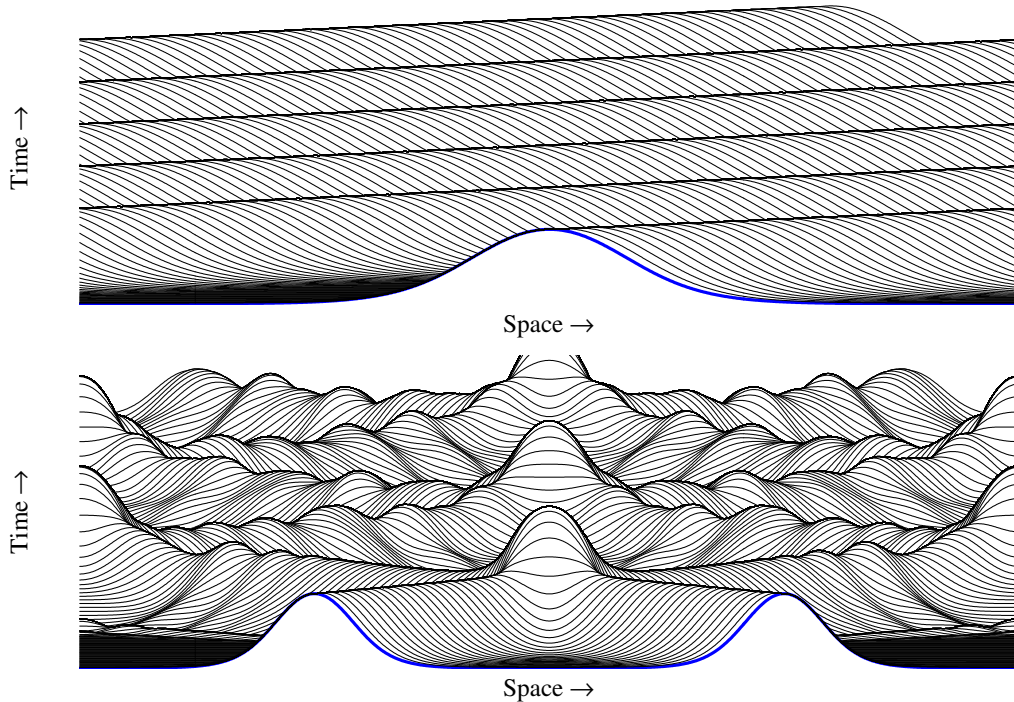


Figure 12. The time slice plots for the case $H_2 = 0$ Eq. (5). The solitary wave solution (top) and interaction of counterpropagating solitary waves (bottom).

The other cases are analysed in detail in [40].

5. Interaction of solitons

In general, a soliton can be described as a stable particle-like state of a nonlinear system [41]. Another way of describing the phenomenon we call soliton is through its properties. A soliton is a wave in the nonlinear environment that (i) has a stable form, (ii) is localised in space and (iii) restores its speed and structure after interaction with another soliton [18, 42]. Solitons emerge when there is a balance in the system between dispersive and nonlinear effects. In essence it can be said that solitons are nonlinear waves that behave between interactions like linear waves. A solitary wave is usually a wave in the nonlinear environment where all the key properties of solitons are not strictly fulfilled. For example, if the interaction between two waves is not entirely elastic (or it is not possible to observe the interaction) or if the form of the wave is not sufficiently stable in time, then the wave is often called a solitary wave to distinguish it from the soliton.

In Fig. 12 one can see the HJ model (5) solitary wave propagation (top) and interaction (bottom). The parameters are the same as in Section 3 except $H_2 = 0$. From Fig. 12 it is clear that while the single HJ pulse is stable it is strictly speaking a solitary wave, not a soliton, because the interaction with another such wave is not elastic as there is significant radiation even during the first interaction event and the shape of the waveprofile is not properly restored after the interaction. However, it should be noted that the parameter combinations can exist where the solitary wave solutions can be relatively stable with almost no radiation.

The ‘time slice’ plot used in Fig. 12 is useful for giving an overview ‘at a glance’ of

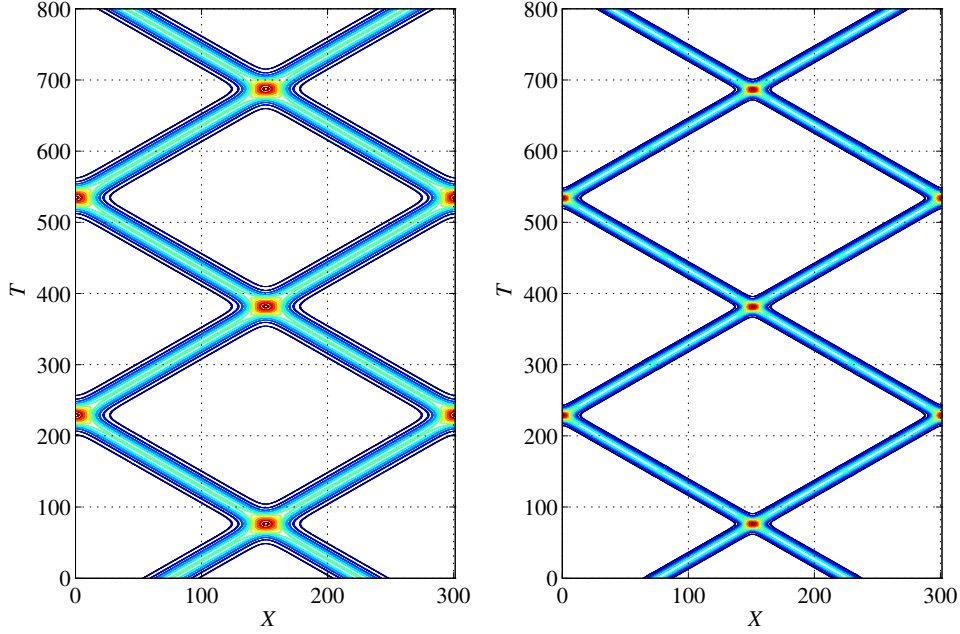


Figure 13. Contour plots of interactions of solitonic solutions. Parameters $c = \pm 0.99$, $P = -10$, $Q = 40$, $H_1 = 1$, $H_2 = 0$ (left) and $H_2 = 0.75$ (right).

the evolution of a solution in time. Spatial coordinate is on the horizontal and time on the vertical axis. Due to the periodic boundary conditions anything moving out of the frame on the left enters the frame on the right.

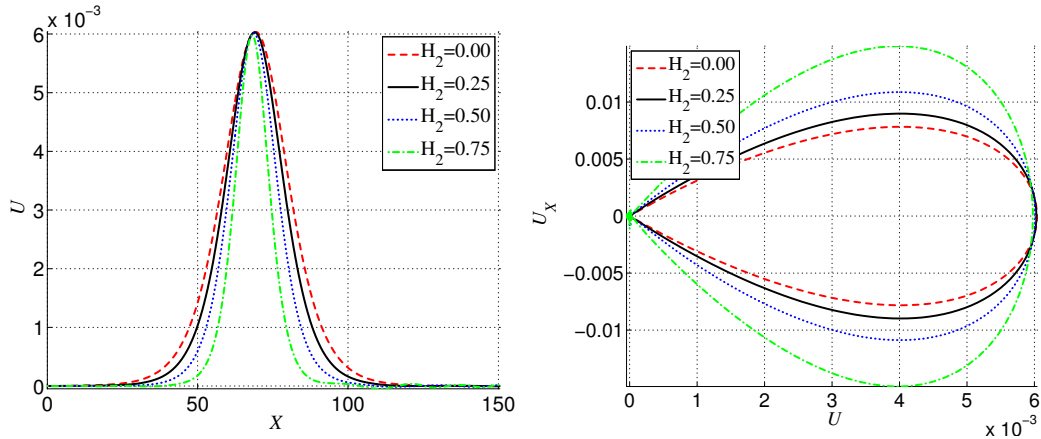


Figure 14. Waveprofile plots (left) and corresponding phase plots (right) at $T = 770$ after five interactions. Parameters $c = \pm 0.99$, $P = -10$, $Q = 40$, $H_1 = 1$. Only a waveprofile propagating to the left is shown.

The interaction of single solitary waves depends on the parameters of the model and consequently, on the dispersion type (normal, anomalous). We start with the following set of parameters: $c = \pm 0.99$, $P = -10$, $Q = 40$, $H_1 = 1$, $H_2 = 0$, $H_2 = 0.25$, $H_2 = 0.50$ and $H_2 = 0.75$. In Fig. 13 one can see the interactions when the parameter $H_2 = 0$ (left) and when $H_2 = 0.75$ (right) – are remarkably similar and non disruptive with the main difference being that the solitonic waveprofiles are more localised if $H_2 \neq 0$. In this case the interactions have almost no radiation (negligible radiation two orders of magnitude smaller than the main pulse amplitude at $\approx 10^{-5}$). Amplitude isolines

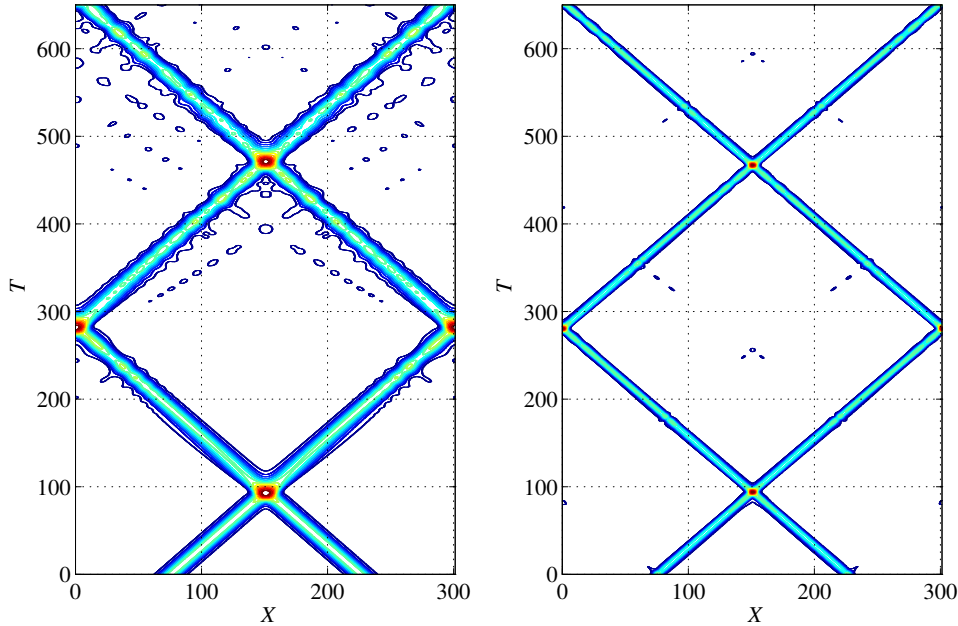


Figure 15. Contour plots of interactions of solitonic solutions. Parameters $c = \pm 0.8$, $P = -10$, $Q = 40$, $H_1 = 4$, $H_2 = 0$ (left) and $H_2 = 5$ (right).

are separated by 0.001 from 0.001 to 0.013 in Fig. 13.

In Fig. 14 waveprofiles and corresponding phase plots after the five interaction events ($T > 700$) are presented. The solitonic waveprofiles corresponding to higher values of H_2 are more localised as expected (the waveprofile in Fig. 14 is propagating to the left). The small distortions to the waveprofiles are easier to spot in phase plots (right), in particular the small radiation close to zero which is noted is two orders of magnitude smaller than the main pulse under the used parameter combination.

Let us return to a parameter set presented in Section 3 for the analytical solution. It turns out that there is also a possible scenario where the solitonic solutions with the additional dispersive term are more stable through interactions than the solitonic solutions if parameter $H_2 = 0$. In Fig. 15 the case $H_2 = 0$ is presented in the left and the case $H_2 = 5$ in the right. The amplitude isolines are separated by 0.02 from 0.02 to 0.3. It is clear that under the parameter set used in Figs 12 and 15 the solitonic waves corresponding to $H_2 = 0$ have greater amount of radiation than the case $H_2 = 5$ which is relatively stable in comparison throughout interactions. Neither of the cases can be considered solitons in the strict mathematical case [18] as in both cases there is significant enough radiation after only three interactions. While unrelated to the mechanics of soliton interactions it is interesting to remark that the used numerical algorithm performs approximately three times faster if $H_2 \neq 0$.

6. Final remarks

The systematic analysis of solutions to the special Boussinesq-type equation with the displacement-dependent nonlinearities has revealed several interesting phenomena. The analysis is focused on Eq. (6) (or its dimensionless form (7)) which is the improved Heimburg-Jackson model for describing the longitudinal wave process in biomembranes. Like every wave equation it describes the process generated by initial

and/or boundary conditions expressed in terms of the dependent variable. Here the variable under consideration is the change of the density in the longitudinal direction. In terms of this variable the existence of solitary solutions is demonstrated, the emergence of trains of solitary pulses is shown and the properties of emergence analysed, and the interaction of single solitary waves and trains studied. We stress that the conventional wave propagation theory involve deformation-dependent nonlinearities while here the governing nonlinear wave equation involves displacement-dependent nonlinearities.

The analysis can be summarised with following conclusions:

- The improved model (Eqs. (6), (7)) removes the discrepancy that at higher frequencies the velocities are unbounded (see Fig. 1);
- The additional dispersive term u_{xxtt} with the coefficient h_2 (or H_2 in the dimensionless form) in addition to the *ad hoc* dispersive term u_{xxxx} [13] describes actually the influence of the inertiality of the microconstituents (lipids) of the biomembrane. This corresponds to the understandings of continuum mechanics of microstructured solids [10] and is demonstrated also experimentally [26]. This term regulates the width of the solitary pulse (see Fig. 6) and such an effect can be used for determining the value of h_2 from experiments. It also determines how fast the transition from the low frequency speeds to the high frequency speeds occurs (see Fig. 1);
- The fourth-order pseudopotential (13) involves several solution types of solitary waves and under certain conditions ($Q > 0$, $H_2 \gg H_1$) an oscillatory solution exists (see Fig. 7);
- Soliton trains can be emerged from an arbitrary initial condition. These results were obtained by numerical simulation by using the pseudospectral method [37]. Depending on the signs of coefficients Q and P , the nonlinear effects start to influence the emergence either from the front or from the back of the propagating pulse (see Fig 10). For the case of a biomembrane one has $Q < 0$, $P > 0$ and the train emerging from a positive input starts with smaller solitons which travel faster than the bigger ones. This is different from the conventional case of nonlinear evolution equations (the KdV equation, for example). In the case of a negative input, the train is headed by bigger solitons which travel faster (see Fig. 10). It has been shown that there are several wave types possible: solitary waves (Fig. 9), oscillatory (Airy-type) waves (Fig. 9), and hybrid solutions.
- The interaction of solitary waves is not fully elastic (see Figs 13, 15) which shows that these solitary waves are not solitons in the strict sense [18]. However, like in other Boussinesq-type equations [3, 12], the radiation effects accompanying every interaction start cumulating rather slowly and the interacting solitons keep their shape for a rather long time. It gives the ground to call emerging solitary waves modelled by Eq. (6) (or Eq. (7)) solitons like it is done in other physical cases [11].

Biological structures as a rule have high complexity because the macrobehaviour is strongly influenced by the embedded microbehaviour. Mathematical modelling is a tool not only for describing biological processes and performing experiments *in silico* but to understand the process. The behaviour of biomembrane is an excellent example how the microstructure (lipids) of a membrane has a direct impact on wave phenomena along the membrane. The analysis of the governing equation (6) (or Eq. (7)) presented above demonstrates the richness of the model from the viewpoint of mathematical physics and opens the ways for physiological experiments concerning the properties of

biomembranes.

Acknowledgement

The valuable comments of the reviewer are acknowledged.

Disclosure statement

No potential conflict of interest was reported by the authors

Funding

This research was supported by the European Union through the European Regional Development Fund (Estonian Programme TK 124) and by the Estonian Research Council (projects IUT 33-24, PUT 434).

References

- [1] J. Boussinesq, *Théorie de l'intumescence liquide, appelée onde solitaire ou de translation, se propageant dans un canal rectangulaire*, Comptes Rendus l'Academie des Sci. 72 (1871), pp. 755–759.
- [2] L. Rayleigh, *On waves*, Philos. Mag. 1 (1876), pp. 257–279.
- [3] C.I. Christov, G.A. Maugin, and A.V. Porubov, *On Boussinesq's paradigm in nonlinear wave propagation*, Comptes Rendus Mécanique 335 (2007), pp. 521–535.
- [4] G.A. Maugin, *On some generalizations of Boussinesq and KdV systems*, Proc. Estonian Acad. Sci. Phys. Math. 44 (1995), pp. 40–55.
- [5] G.A. Maugin, *Nonlinear Waves in Elastic Crystals*, Oxford University Press, Oxford, 1999.
- [6] A.V. Porubov, *Amplification of Nonlinear Strain Waves in Solids*, World Scientific, Singapore, 2003.
- [7] A. Berezovski, J. Engelbrecht, A. Salupere, K. Tamm, T. Peets, and M. Berezovski, *Dispersive waves in microstructured solids*, Int. J. Solids Struct. 50 (2013), pp. 1981–1990.
- [8] J. Engelbrecht, K. Tamm, and T. Peets, *On mathematical modelling of solitary pulses in cylindrical biomembranes*, Biomech. Model. Mechanobiol. 14 (2015), pp. 159–167.
- [9] J. Engelbrecht, *Nonlinear Wave Dynamics. Complexity and Simplicity.*, Kluwer, Dordrecht, 1997.
- [10] R.D. Mindlin, *Micro-structure in linear elasticity*, Arch. Ration. Mech. Anal. 16 (1964), pp. 51–78.
- [11] G.A. Maugin, *Solitons in elastic solids (1938-2010)*, Mech. Res. Commun. 38 (2011), pp. 341–349.
- [12] J. Engelbrecht, A. Salupere, and K. Tamm, *Waves in microstructured solids and the Boussinesq paradigm*, Wave Motion 48 (2011), pp. 717–726.
- [13] T. Heimburg and A.D. Jackson, *On soliton propagation in biomembranes and nerves.*, Proc. Natl. Acad. Sci. USA 102 (2005), pp. 9790–5.
- [14] S.S.L. Andersen, A.D. Jackson, and T. Heimburg, *Towards a thermodynamic theory of nerve pulse propagation.*, Prog. Neurobiol. 88 (2009), pp. 104–13.

- [15] R. Appali, U. Van Rienen, and T. Heimbürg, *A comparison of the Hodgkin-Huxley model and the soliton theory for the action potential in nerves*, in *Adv. Planar Lipid Bilayers Liposomes, Vol. 16*, A. Iglic, ed., chap. 9, Academic Press, 2012, pp. 275–299.
- [16] J.K. Mueller and W.J. Tyler, *A quantitative overview of biophysical forces impinging on neural function.*, *Phys. Biol.* 11 (2014), p. 051001.
- [17] N. Zabusky and M. Kruskal, *Interaction of “solitons” in a collisionless plasma and the recurrence of initial states*, *Phys. Rev. Lett.* 15 (1965), pp. 240–243.
- [18] P. Drazin and R. Johnson, *Solitons: and Introduction*, Cambridge University Press, Cambridge, 1989.
- [19] A. Salupere, P. Peterson, and J. Engelbrecht, *Long-time behaviour of soliton ensembles . Part I – Emergence of ensembles*, *Chaos, Solitons & Fractals* 14 (2002), pp. 1413–1424.
- [20] D. Debanne, E. Campanac, A. Bialowas, E. Carlier, and G. Alcaraz, *Axon physiology*, *Physiol. Rev.* 91 (2011), pp. 555–602.
- [21] A.L. Hodgkin and A.F. Huxley, *A quantitative description of membrane current and its application to conduction and excitation in nerve*, *J. Physiol.* 117 (1952), pp. 500–544.
- [22] K. Iwasa, I. Tasaki, and R. Gibbons, *Swelling of nerve fibers associated with action potentials*, *Science* 210 (1980), pp. 338–339.
- [23] I. Tasaki, *A macromolecular approach to excitation phenomena: mechanical and thermal changes in nerve during excitation*, *Physiol. Chem. Phys. Med. NMR* 20 (1988), pp. 251–268.
- [24] T. Heimbürg and A. Jackson, *On the action potential as a propagating density pulse and the role of anesthetics*, *Biophys. Rev. Lett.* 2 (2007), pp. 57–78.
- [25] F. Maurin and A. Spadoni, *Wave propagation in periodic buckled beams. Part I: Analytical models and numerical simulations*, *Wave Motion* 66 (2016), pp. 190–209.
- [26] F. Maurin and A. Spadoni, *Wave propagation in periodic buckled beams. Part II: Experiments*, *Wave Motion* 66 (2016), pp. 210–219.
- [27] M.J. Ablowitz, *Nonlinear Dispersive Waves. Asymptotic Analysis and Solitons.*, Cambridge Univ Press, Cambridge, 2011.
- [28] T. Kakutani, and N. Yamasaki, *Solitary Waves on a Two-Layer Fluid.*, *J. Phys. Soc. Jpn.* 45 (1978), pp. 674–679.
- [29] A.V. Slyunyaev and E.N. Pelinovski, *Dynamics of large-amplitude solitons.*, *J. Exp. Theor. Phys.* 116 (1999), pp. 173–181.
- [30] T. Peets, K. Tamm, and J. Engelbrecht, *On the role of nonlinearities in the Boussinesq-type wave equations*, *Wave Motion*, in press.
- [31] B. Lautrup, R. Appali, A.D. Jackson, and T. Heimbürg, *The stability of solitons in biomembranes and nerves.*, *Eur. Phys. J. E. Soft Matter* 34 (2011), pp. 1–9.
- [32] T. Peets and K. Tamm, *On mechanical aspects of nerve pulse propagation and the Boussinesq paradigm*, *Proc. Estonian Acad. Sci.* 64 (2015), pp. 331–337.
- [33] K. Tamm and T. Peets, *On solitary waves in case of amplitude-dependent nonlinearity*, *Chaos, Solitons & Fractals* 73 (2015), pp. 108–114.
- [34] T. Peets, K. Tamm, and J. Engelbrecht, *Numerical investigation of mechanical waves in biomembranes*, in *Conf. Proc. YIC GACM 2015 3rd ECCOMAS Young Investig. Conf. 6th GACM Colloquium, July 20-23, 2015, Aachen, Ger.*, S. Elgeti and J.W. Simon, eds. 2015, pp. 1–4.
- [35] B. Fornberg and D.M. Sloan, *A review of pseudospectral methods for solving partial differential equations*, *Acta Numer.* 3 (1994), p. 203.
- [36] B. Fornberg, *A Practical Guide to Pseudospectral Methods*, Cambridge University Press, Cambridge, 1998.
- [37] A. Salupere, *The pseudospectral method and discrete spectral analysis*, in *Appl. Wave Math.*, E. Quak and T. Soomere, eds., Springer Berlin Heidelberg, Berlin, 2009, pp. 301–334.
- [38] E. Jones, T. Oliphant, and P. Peterson, *SciPy: open source scientific tools for Python* (2007). Available at <http://www.scipy.org>.
- [39] A. Hindmarsh, *ODEPACK, a Systematized Collection of ODE Solvers*, Vol. 1, North-

Holland, Amsterdam, 1983.

- [40] J. Engelbrecht, K. Tamm, and T. Peets, *On solutions of a Boussinesq-type equation with amplitude-dependent nonlinearities: the case of biomembranes*, arXiv:1606.07678 [nlin.PS] (2016).
- [41] R. Dodd, J. Eilbeck, J. Gibbon, and H. Morris, *Solitons and nonlinear wave equations*, Academic Press Inc. LTD., London, 1982.
- [42] J. Engelbrecht, *Beautiful dynamics*, Proc. Estonian Acad. Sci. Physics/Mathematics 1 (1995), pp. 108–119.